

# Digitally Fabricated Keyed Concrete Connections

**Conference Paper****Author(s):**

[Bischof, Patrick](#) ; [Mata Falcón, Jaime](#) ; [Burger, Joris Jan](#) ; [Kaufmann, Walter](#) 

**Publication date:**

2022

**Permanent link:**

<https://doi.org/10.3929/ethz-b-000557503>

**Rights / license:**

[In Copyright - Non-Commercial Use Permitted](#)

**Originally published in:**

RILEM Bookseries 37, [https://doi.org/10.1007/978-3-031-06116-5\\_36](https://doi.org/10.1007/978-3-031-06116-5_36)

**Funding acknowledgement:**

141853 - Digital Fabrication - Advanced Building Processes in Architecture (SNF)



# Digitally Fabricated Keyed Concrete Connections

Patrick Bischof<sup>1</sup> , Jaime Mata-Falcón<sup>1</sup> , Joris Burger<sup>2</sup> ,  
and Walter Kaufmann<sup>1</sup>

<sup>1</sup> Institute of Structural Engineering, Department of Civil, Environmental and Geomatic Engineering, ETH Zurich, 8093 Zurich, Switzerland  
bischof@ibk.baug.ethz.ch

<sup>2</sup> Institute of Technology in Architecture, Department of Architecture, ETH Zurich, 8093 Zurich, Switzerland

**Abstract.** Most current technologies in digital fabrication with concrete (DFC) rely on controlled environmental conditions and, thus, have been used in prefabricated construction. Prefabricated reinforced concrete elements produced in factories need assembly and connection on-site. Using DFC for producing tailor-made geometries and applying surface roughness generates new possibilities for the design of connections. DFC enables (i) fabricating dry connections, for example, by using exact formworking or milling processes, and (ii) the relatively straightforward preparation of rough construction joints, for example, by using extrusion processes. In a recent study, a series of different specimens incorporating connections were tested using deformation-controlled push-off tests. This contribution presents the experimental campaign including design, preparation and test results employing keyed connections produced with the *Eggshell* technology, a fabrication process using 3D printed thin plastic formwork.

**Keywords:** Digital fabrication with concrete · Prefabricated construction · Connections · Shear keys · Eggshell

## 1 Introduction

Digital fabrication refers to fabrication methods directly following model data. Advantages of digital fabrication with concrete (DFC) include the possibility of creating non-standard shapes without a significant influence on the fabrication cost and time. This advantage renders new possibilities for producing structural connections [1, 2] by shaping tailored surfaces, e.g. with robotically produced formworks, or by post-processing printed surfaces by milling or cutting of set-on-demand concrete in 3D printing processes, e.g. [3]. Connections are a critical aspect when exploiting DFC for fostering sustainability in the construction industry, given the current dependency of DFC on controlled fabrication conditions, i.e. prefabrication, and existing transport constraints. Structural connections serve for transferring compressive, shear and tensile stresses between adjacent elements, members, or parts thereof (e.g. between a topping or a lost formwork and

cast concrete). Furthermore, they may facilitate the assembly of precast elements (cf. keyed connections in precast segmental bridges).

The load-bearing capacity of keyed connections mainly depends on the frictional resistance between contact surfaces and on the interlocking resistance of the keys [4]. The frictional resistance relies on the roughness of the surface and the compressive stress prevailing in the joint. The performance of a shear key is governed by its geometry, i.e., key length, depth and inclination. Connections with several keys must fit with small tolerances to ensure (i) their combined contribution to the load-bearing capacity and (ii) the targeted alignment in the assembly. Accordingly, the production of such connections is challenging.

This contribution addresses the design, fabrication and structural testing of fitting keyed connections with the DFC technology *Eggshell* [5]. *Eggshell* is a concrete pre-fabrication process that uses robotic fused deposition modelling (FDM) 3D printing of thin plastic formworks combined with set-on-demand concrete casting. The presented test series investigates the performance of shear keys with smaller dimensions than typically used in conventional construction where larger aggregate sizes are common. The AASHTO design guide [6] recommends using key depths larger than twice the maximum aggregate size, while the EN 1992-1-1 [4] recommends a minimum key depth of merely 5 mm. However, small key depths are beneficial for slender building members, facilitating the assembly of precast elements and adjusting to flexible element geometries, which are all typical design constraints of DFC elements.

## 2 Digitally Fabricated Connections: Materials and Methods

### 2.1 Test Setup

The shear performance of several configurations of keyed concrete connections was tested with the push-off test setup shown in Fig. 1a. The vertical load was increased with a displacement-controlled rate of 0.12 mm/min, while the horizontal compression was constant at 2 MPa during the test. The setup for applying the horizontal compression was decoupled from the specimens by vertically supported steel plates and PTFE sheets, avoiding any contribution of inclined rods to the resistance of the connection.

### 2.2 Specimen Design

The push-off specimens consisted of two L-shaped pieces: One piece hosted an insert with the keyed connection, while the other piece was match-cast to the keyed joint (see Fig. 1a). The complete specimens featured a width of 300 mm, a height of 400 mm, and a thickness of 120 mm. The nominal contact surface of the joint was 200 mm × 120 mm. The inserts had nominal dimensions of 200 mm × 120 mm × 80 mm. The host and the contact pieces were cast with an ultra high performance fibre reinforced concrete (UHPC) with higher compressive and tensile strength, ensuring failure in the inserts.

The presented experimental campaign included eight key configurations varying (i) the key dimension  $d_{key} = \{25, 50, 100\}$  mm, (ii) the key depth  $h_{key}$  by fixing the ratio of key depth to key length to 1:5, (iii) the number of keys (1 or 2), and (iv) the formwork

printing direction (H = horizontal or V = vertical, see Sect. 2.4). All specimens presented in this study were *Eggshell*-printed dry connections (designation ED) and are further denominated in the following according to their configurations: e.g. Specimen ED2V50 had 2 keys, vertically printed formwork (V), a key dimension  $d_{key} = 50$  [mm].

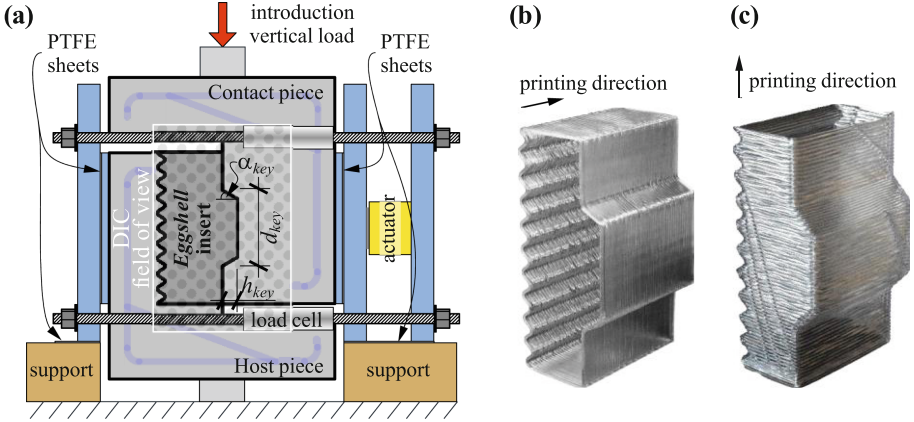


**Fig. 1.** Presentation of the test setup: (a) test setup, (b) formwork of *Eggshell* insert printed horizontally, (c) formwork of *Eggshell* insert printed vertically.

### 2.3 Material Properties

The concrete mix of the *Eggshell*-inserts corresponded to the one used by Burger et al. [5] with a maximum aggregate size of 4 mm. The compressive cylinder strength amounted to  $f_{cm} = 80.2$  MPa (average of two cylinder tests), while the tensile strength was  $f_{ctm} = 3.2$  MPa (average of two double-punch tests [7]). The hosting pieces of the specimen made of UHPFRC provided a compressive strength of  $f_{cm} = 167.7$  MPa and tensile strength of  $f_{ctm} = 13.3$  MPa.

### 2.4 Specimen Production with *Eggshell* Technology

The inserts were produced using the *Eggshell* fabrication setup (described in [5]) for their formwork. The production of the inserts consisted of the following steps, illustrated in Fig. 2: (i) formwork design, (ii) print path generation, (iii) 3D printing with a thermoplastic PET-G filament of diameter 2.85 mm (nozzle diameter of 1.5 mm), (iv) set-on-demand casting, and (v) demoulding. Note that the insert formworks were either printed horizontally or vertically, leading to a different orientation of the filaments with respect to the joint ( $\alpha_{key} = 26.5^\circ$  (1.2) in horizontal printing, see Fig. 1b, and  $\alpha_{key} = 45^\circ$  in vertical printing, Fig. 1c, respectively) and a slightly different roughness.

The casting rate was 240 mm/h, pouring a batch of accelerated concrete with a height of 20 mm every 5 min. After curing, the samples were demoulded using a heat gun and pliers. Finally, the inserts were placed inside an L-shaped conventional timber formwork

to produce the host piece (Fig. 1a). The contact piece was match-cast against the insert, using a conventional formwork for the remaining sides.

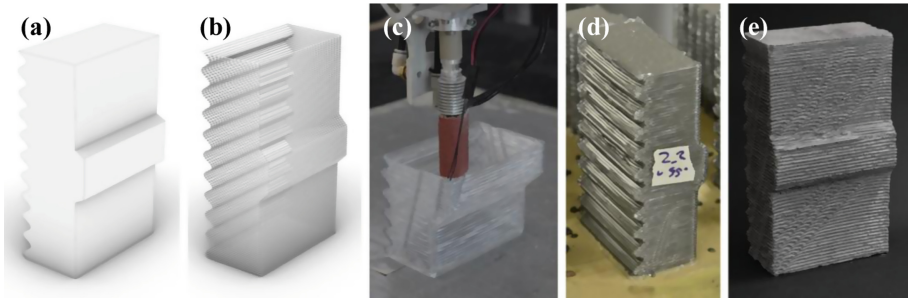


**Fig. 2.** Design-to-fabrication process of the inserts. (a) 3D model of the formwork, (b) formwork toolpath, (c) 3D formwork printing, (d) casting, (e) concrete insert after formwork removal.

3D printing overhangs with FDM is challenging. For the vertically printed inserts, the key angle ( $\alpha_{key}$ ) was limited to  $45^\circ$  for minimising the geometrical tolerances, even though previous experiments [5] proved the feasibility of achieving overhangs up to  $60^\circ$  by modifying the flow rate during the print. While the geometrical imprecision of the inserts was below 3 mm, a printed formwork with stiffening ribs would minimise it further. Accordingly, it would be feasible to produce either two separate but fitting pieces or a piece fitting to an existing surface geometry (e.g. in an existing building).

## 2.5 Instrumentation

Load cells were employed to measure the global vertical force (testing machine's built-in load cell) and the horizontal force (four load cells on each of the four rods, see Fig. 1a). High-resolution 3D digital image correlation (VIC-3D system from Correlated Solutions) was applied for obtaining full-field deformations, which served to evaluate (i) the joint and crack kinematics and (ii) the principal strains at the key. The chosen configuration captured a field of  $225 \text{ mm} \times 150 \text{ mm}$  on the specimen's speckled surface (see Fig. 1, speckle size = 0.18 mm). The resolution was  $\approx 0.04 \text{ mm/px}$ .

The automated crack detection and measurement approach (ACDM, [8]) was used to determine the joint kinematics. The joint slip was evaluated continuously along the joint by assuming two rigid crack lips, each with a distance of 7.5 mm from the joint surface. The strain field was computed from the displacement field, considering a small virtual gauge length of 1.8 mm. The principal compressive strains and their directions served to study the load introduction in the interlocking key in detail.

## 3 Digitally Fabricated Connections: Results

Figure 3a shows the vertical nominal shear stress  $\tau_{nom}$  and the shear force  $V$ , respectively, against the average crack slip  $\delta_s$  along the joint length for five of the tested eight specimens, i.e., Specimens ED1V100, ED1V50, ED1H50, ED2V50, ED1V25; the behaviour

of Specimen EDH50 is representative for the remaining specimens with horizontally printed formwork. Figure 3b shows the principal compressive strains  $\varepsilon_2$  (solid lines) and their direction  $\varphi_2$  (dashed lines), respectively, against the average crack slip  $\delta_s$  for Specimens ED1V100 (red), ED1V50 (violet), and ED1V25 (green).

The  $\tau_{nom} - \delta_s$  curve features three distinct phases: The first phase is described by the frictional resistance of the key until a diagonal crack opens at the edge of the loaded end of the key (○ in Fig. 3a). In the second phase, the interlocking key clearly contributes to the overall load-carrying capacity. In this phase, the principal compressive strain direction reorients towards the direction of the load introduction ( $\varphi_2 = 75^\circ \dots 90^\circ$  in Fig. 3b for ED1V100 and ED1V50) for the specimens whose key is activated. After shearing off the key (x in Fig. 3a), the applied load corresponds to the joint's frictional resistance, continuously decreasing with increasing joint slip.

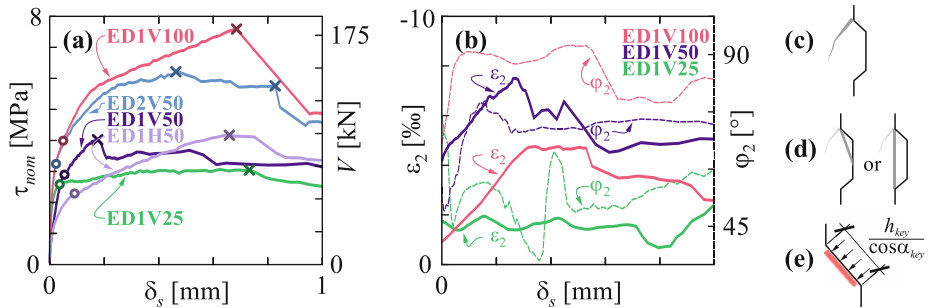


**Fig. 3.** Evaluation of pull-out tests on DFC keyed connections: (a) nominal shear stress  $\tau_{nom}$  or shear resistance  $V$  against crack slip  $\delta_s$ , (b) principal compressive strains  $\varepsilon_2$  and their directions  $\varphi_2$  against crack slip  $\delta_s$ , (c) occurrence of crack (marked with ○ in (a)), (d) key failure (marked with x), (e) evaluated area (red) for  $\varepsilon_2$  and  $\varphi_2$ .

The frictional resistance controlled the load-bearing capacity of the specimens with one key with the smallest tested dimensions ( $h_{key} = 25$  mm). The keyed connections with larger height proved an increasing interlocking effect with increasing key dimensions (+25% with  $h_{key} = 50$  mm and +150% with  $h_{key} = 100$  mm, both compared to  $h_{key} = 25$  mm). The peak compressive strain at the key reached  $-8\%$  for the specimens with exploited interlocking key (see ED1V50 in Fig. 3b).

Generally, the frictional resistance was – expectedly – higher for the specimens with vertically printed formwork, as the formwork's printed filaments, oriented perpendicularly to the tangential force component, provided a higher roughness in this direction. On the other hand, the horizontally printed formwork incorporated keys with a smaller key angle  $\alpha_{key}$ , resulting in a slightly superior shear resistance, as revealed by comparing specimens ED1H50 and ED1V50.

## 4 Conclusion and Outlook

Digital fabrication with concrete (DFC) allows producing tailor-made geometries and surface roughness. Accordingly, it brings about new three-dimensional possibilities for the design of concrete connections between adjacent elements, members, or parts thereof. This contribution discusses digitally fabricated keyed connections for prefabricated construction. Several configurations of keyed connections were tested with a push-off test setup for their resistance against shear stresses.

The tested keyed connections proved an increasing interlocking effect with larger key dimensions and steeper key angles. The smallest tested key dimensions (one key with a depth of 5 mm, i.e., roughly 1.25 times the maximum aggregate size) did not contribute to the overall load-bearing capacity. The latter observation should be further investigated for connections incorporating several small keys, especially for loading conditions leading to cross-sectional strain gradients, as prevailing under combined shear forces and bending moments.

**Acknowledgements.** The authors thank Armin Bratschi, Siro Gianinazzi, and the IBK Structural Lab personnel for their support in this research project, which is supported by the NCCR in Digital Fabrication and funded by the SNSF [project number 51NF40 141853].

## References

1. Bischof, P., Mata-Falcón, J., Kaufmann, W.: Fostering innovative and sustainable mass-market construction using digital fabrication with concrete. Submitted to *Cement and Concrete Research* (2022)
2. Baghdadi, A., Meshkini, A., Kloft, H.: Inspiration of interlocking wooden puzzles for precast concrete construction. In: *Proceedings of the International fib Symposium on the Conceptual Design of Structures*, Switzerland, pp. 531–538. Attisholz Areal, Switzerland (2021)
3. Hack, N., Kloft, H.: Shotcrete 3D printing technology for the fabrication of slender fully reinforced freeform concrete elements with high surface quality: a real-scale demonstrator. In: Bos, F.P., Lucas, S.S., Wolfs, R.J.M., Salet, T.A.M. (eds.) *DC 2020. RB*, vol. 28, pp. 1128–1137. Springer, Cham (2020). [https://doi.org/10.1007/978-3-030-49916-7\\_107](https://doi.org/10.1007/978-3-030-49916-7_107)
4. EN 1992-1-1: Eurocode 2: Design of concrete structures - Part 1-1: General rules and rules for buildings (2004)
5. Burger, J., et al.: Eggshell: ultra-thin three-dimensional printed formwork for concrete structures. *3D Printing Addit. Manuf.* **7**, 48–59 (2020). <https://doi.org/10.1089/3dp.2019.0197>
6. AASHTO: Guide Specification for Design and Construction of Segmental Concrete Bridges, 2nd edn. (1999)
7. Marti, P.: Size effect in double-punch tests on concrete cylinders. *MJ* **86**, 597–601 (1989). <https://doi.org/10.14359/2261>
8. Gehri, N., Mata-Falcón, J., Kaufmann, W.: Automated crack detection and measurement based on digital image correlation. *Constr. Build. Mater.* **256**, 119383 (2020). <https://doi.org/10.1016/j.conbuildmat.2020.119383>